

The Synergy with *SPICA* and ALMA — for a Robust AGN Diagnostic —

TAKUMA IZUMI,¹ KOTARO KOHNO,^{1,2} AND NOZOMU KAWAKATU³

¹*Institute of Astronomy, The University of Tokyo, Japan*

²*Research Center for the Early Universe, The University of Tokyo, Japan*

³*Kure National College of Technology, Japan*

ABSTRACT

Here we show the results of our ALMA cycle 0 observation toward the nearby type-1 Seyfert nucleus in NGC 1097. We observed some typical dense gas tracers such as HCN ($J=4-3$) and HCO⁺ ($J=4-3$). We find that the HCN ($J=4-3$)/HCO⁺ ($J=4-3$) and HCN ($J=4-3$)/CS ($J=7-6$) integrated intensity ratios are enhanced in AGNs including NGC 1097 compared to nearby starburst galaxies and Galactic star forming regions. Multi-line/transition analysis of HCN and HCO⁺ emissions reveal that these lines are emitted from dense ($10^{4.5} \leq n_{\text{H}_2} [\text{cm}^{-3}] \leq 10^6$) and hot ($70 \leq T_{\text{kin}} [\text{K}] \leq 550$) regions, and that HCN to HCO⁺ abundance ratio is high (4–20). We introduce a “high-temperature chemistry” to explain the observed properties. Finally, we briefly discuss the possible future studies with ALMA and *SPICA* on AGN science.

1. INTRODUCTION

How did galaxies evolve to form their wide physical/chemical variety observed today? This is one of the essential problems in modern astronomy. Especially, a supermassive black hole in the center of a galaxy is known to coevolve with its host galaxy (e.g., Kormendy & Ho 2013), although the mechanism of the coevolution is unknown. To study these problems, it is necessary to reveal how some powerful heating mechanisms such as active galactic nuclei (AGNs) and starbursts (SBs) affect each other, and also their host galaxies. However, prior to study the effect of each heating mechanism, we have to construct a robust method to diagnose such mechanisms observationally. Historically, optical and IR astronomy have presented many sophisticated diagnostic methods utilizing the different physical/chemical properties of atomic lines. However, these wavelengths suffer dust extinction and thus can not penetrate deep into the dusty nuclei in e.g., ultra-luminous infrared galaxies = ULIRGs.

This problem of dust extinction can be overcome in mm/submm wavelengths. Based on this perspective, we have identified HCN-enhancement in intensity with respect to, e.g., HCO⁺ and CO, as the most promising indicator of AGNs (e.g., Kohno 2005). However, the cause of this HCN-enhancement is not clear because many different processes can contribute to the phenomenon in active environments, including high gas densities, high temperatures, and/or non-standard molecular abundances. In addition to these causes, a non-collisional excitation such as IR-pumping by the re-radiation from UV/X-ray heated dust can produce vibrationally excited lines and severely affect the rotational lines, which makes it difficult to deal the line intensities qualitatively.

To discuss the cause of the HCN-enhancement in detail, we observed the nuclear region of the nearby ($D = 14.5$ Mpc) Seyfert galaxy NGC 1097 by submillimeter dense gas tracers such as HCN ($J=4-3$) and HCO⁺ ($J=4-3$) by the *Atacama Large Millimeter/submillimeter Array* (ALMA). This galaxy hosts a type-1 Seyfert nucleus, though it is a low luminous one ($L_{2-10\text{keV}} = 4.4 \times 10^{40} \text{ erg s}^{-1}$, $L_{\text{bol}} = 8.6 \times 10^{41} \text{ erg s}^{-1}$ at $D = 14.5$ Mpc; Nemmen et al. 2006). This nucleus is surrounded by a brilliant SB ring with a radius of ~ 700 pc, which is luminous at various wavelengths. The molecular condensation at the nucleus shows elevated HCN to HCO⁺ integrated intensity ratio ($\equiv R_{\text{HCN}/\text{HCO}^+}$) of ~ 2 for both $J=1-0$ (Kohno et al. 2003) and $3-2$ (Hsieh et al. 2012) transitions, suggesting that the physical/chemical properties would be dominated by the AGN in this nucleus. Here, we show a digest of the results of our observations in this paper. The details are extensively discussed in Izumi et al. (2013).

2. OBSERVATION

We observed NGC 1097 with the band 7 (~ 350 GHz) receiver on ALMA using the 2SB dual-polarization setup, in the cycle 0 (ID=2011.0.00108.S, PI: K. Kohno). The observation was performed in a compact configuration and the total observing time was ~ 2.1 hrs including overheads. Weather conditions were good throughout the observation with a system temperature of 150–200 K. The image reconstruction was done with the task CLEAN in CASA and analyzed with MIRIAD both in standard manners. Using natural weighting, the achieved synthesized beam is $1''.5 \times 1''.2$, P.A. = -72.4 deg for HCN ($J=4-3$), for example. This angular resolution (corresponds to ~ 100 pc) is enough to separate the emission from the AGN and the circumnuclear SB ring in NGC 1097. Achieved rms noises are ~ 2.1 mJy beam⁻¹ and ~ 2.3 mJy beam⁻¹ in the LSB and the USB, at velocity resolutions of 8.6 km s^{-1} and 8.3 km s^{-1} , respectively.

IZUMI ET AL.

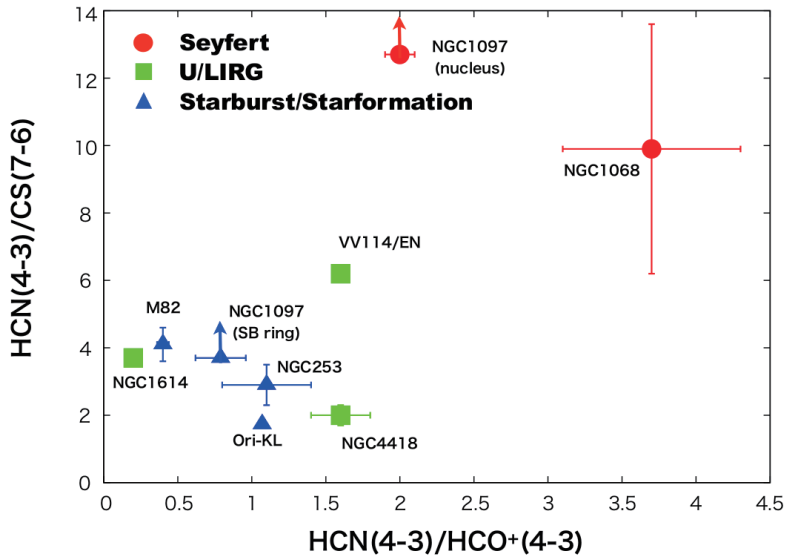


Figure 1. HCN ($J=4-3$) to HCO^+ ($J=4-3$) and HCN ($J=4-3$) to CS ($J=7-6$) integrated intensity ratios of various environments in brightness temperature scale. Only NGC 1097 and NGC 1068 (both are AGN-host galaxies) exhibit enhanced HCN ($J=4-3$) emission with respect to HCO^+ ($J=4-3$) and CS ($J=7-6$).

3. NEW MOLECULAR LINE DIAGNOSTICS: $R_{\text{HCN}/\text{HCO}^+}$ VS. $R_{\text{HCN}/\text{CS}}$

Among several line emissions in band 7, we focus on the extremely high HCN ($J=4-3$) to CS ($J=7-6$) integrated intensity ratio ($R_{\text{HCN}/\text{CS}}$), which is >12.7 in brightness temperature scale. In addition, the HCN ($J=4-3$) to HCO^+ ($J=4-3$) integrated intensity ratio ($R_{\text{HCN}/\text{HCO}^+}$) is also high (~ 2.1) in this nucleus, which is the same trend as the low- J transitions (Kohno et al. 2003). We searched the literature (Bayet et al. 2008, 2009; Iono et al. 2013; Imanishi & Nakanishi 2013; Knudsen et al. 2007; Pérez-Beaupuits et al. 2009; Schilke et al. 1997; Seaquist & Frayer 2000) to check whether such a ratio is commonly observed or not, and the results are summarized in Figure 1. Note that one advantage of this diagram over the previous diagnostic diagram using HCN ($J=1-0$) line (Kohno 2005) is that it is much more applicable to high redshift galaxies because its lines are still within the frequency coverage of ALMA up to redshift $z \sim 3$.

At first inspection, we find that SB galaxies, Galactic star forming regions, and SB-dominated ULIRG (NGC 1614) are located in the bottom-left region of the diagram. On the other hand, the two AGN-host galaxies, NGC 1097 and NGC 1068, are located in the top-right, although NGC 1097 has a compact nuclear star-forming region and the low angular resolutions of the NGC 1068 observations are likely contaminated by the circumnuclear SB ring. VV114 East Nucleus (ULIRG/AGN+SB) shows somewhat higher ratios than those in SB galaxies. Therefore, from this diagram, one might deduce that a galaxy which has a larger AGN contribution tends to reside in the top-right region more. However, this is a tentative view as we do not have clear theoretical evidence to support the use of this diagram, and it is based on a few samples. Therefore, we need large samples and theoretical models to test extensively this diagram. Note that NGC 4418 shows line ratios comparable to those in SB galaxies, though the energy budget in the nuclear region of NGC 4418 seems to be dominated by a buried AGN (Imanishi et al. 2004; Spoon et al. 2001). One possible explanation for this situation would be IR-pumping, which could significantly affect the molecular rotational populations. Actually, a clear absorption feature of HCN at $14.0 \mu\text{m}$ and a vibrationally excited HCN emission are detected in this nucleus (Lahuis et al. 2007; Sakamoto et al. 2010).

4. NON-LTE EXCITATION ANALYSIS IN THE NUCLEUS

To reveal the cause of the HCN-enhancement, we investigated the physical conditions (gas density = n_{H_2} , kinetic temperature = T_{kin} , and abundance (we estimate it by using the molecular column density = N_{mol})) of typical dense gas tracers, HCN and HCO^+ , by using RADEX (van der Tak et al. 2007). RADEX uses an escape probability approximation to solve the non-LTE excitation in a homogeneous (single temperature, single density), single component medium. Here, we used the $J=4-3$ (this work) and $3-2$ (Hsieh et al. 2012) transitions of HCN and HCO^+ for the simulation.

To conduct the simulation, we varied the gas kinetic temperature within a range of $T_{\text{kin}} = 10-600 \text{ K}$ ($dT_{\text{kin}} = +10 \text{ K}$), and a gas density of $n_{\text{H}_2} = 10^2-10^7 \text{ cm}^{-3}$ ($dn_{\text{H}_2} = \times 10^{0.25}$). In addition, a ratio of gas density to velocity gradient, or equivalently gas column density to line velocity width, was changed as $N_{\text{HCO}^+}/dV [\text{cm}^{-2} (\text{km s}^{-1})^{-1}] = 2.0 \times 10^9$ to 2.0×10^{14} , and HCN to HCO^+ abundance ratio ($[\text{HCN}]/[\text{HCO}^+]$) was changed as 1, 2, ..., 15, 20, 30, ..., 100. The $T_{\text{bg}} = 2.73 \text{ K}$ background emission was also added to the calculation. Under these conditions, we ran RADEX and then carried out χ^2 tests to search for the best parameters to reproduce the observed intensity ratios.

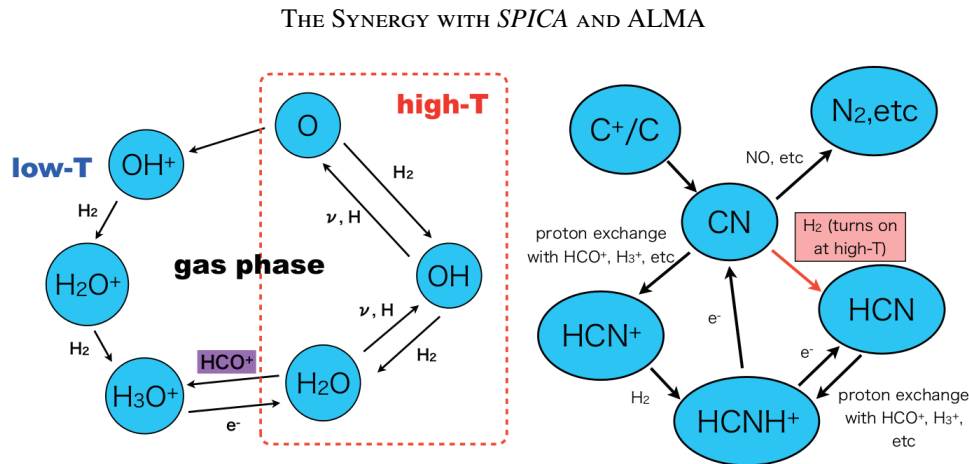


Figure 2. A schematic picture of the high temperature gas phase chemistry especially about H_2O (left) and HCN (right). These molecules are effectively formed as the temperature gets higher.

As a result, we conclude that these HCN and HCO^+ emissions come from hot ($70 \leq T_{\text{kin}} [\text{K}] \leq 550$) and dense ($10^{4.5} \leq n_{\text{H}_2} [\text{cm}^{-3}] \leq 10^6$) molecular clouds, where the $[\text{HCN}]/[\text{HCO}^+]$ is enhanced to 4–20.

5. INTERPRETATION OF OUR RESULTS — FROM MOLECULAR GAS PHASE CHEMISTRY

One possible interpretation of our results is based on a “high temperature chemistry” (Figure 2), which has been proposed in, e.g., Harada et al. (2010). This kind of chemistry suggests that the abundance of H_2O is enhanced in high temperature environments, especially at $T \geq 300 \text{ K}$, by the hydrogenation of atomic O. Thus the abundances of O and/or OH are suppressed in such hot regions. The fractional abundances of our interested molecules under such conditions are discussed below.

HCN: The hydrogenation from CN with H_2 , $\text{CN} + \text{H}_2 \rightarrow \text{HCN} + \text{H}$, is an endothermic reaction which has a relatively low reaction barrier of $\gamma = 820 \text{ K}$, thus the HCN abundance is effectively enhanced in high temperature environments. Also, the decrease in O atom due to the formation of water would lead to relatively carbon-rich conditions, which would also act to enhance HCN abundance.

HCO^+ : This ion species is generally created as $\text{CO} + \text{H}_3^+ \rightarrow \text{HCO}^+ + \text{H}_2$. However, after the temperature increases and the creation of water and HCN are promoted, protonated species of these molecules tend to take up much of the positive charge in the form of H_3O^+ and HCNH^+ , rather than H_3^+ and HCO^+ , by reactions of, for example, $\text{H}_2\text{O} + \text{H}_3^+ \rightarrow \text{H}_3\text{O}^+ + \text{H}_2$, $\text{H}_2\text{O} + \text{HCO}^+ \rightarrow \text{H}_3\text{O}^+ + \text{CO}$. These reactions would prevent the HCO^+ formation and/or decrease the HCO^+ abundance.

As described above, the enhanced HCN abundance with respect to HCO^+ , which can explain the observed AGN-specific properties, can be expected in high temperature environments. However, it is doubtful whether such a low-luminosity AGN in NGC 1097 can heat the surrounding ISM to several hundred kelvin at a tens of parsec scale. Probably, we should expect non-radiative heating mechanism such as shock waves associated with the AGN (jet or outflow) to be important in heating the gas in this nucleus, though such a jet component or a sign of shock heating has not been observed so far. Clearly, we need an observation with higher angular resolution and sensitivity.

6. SUMMARY AND FUTURE PROSPECTS WITH *SPICA*

In this paper, we present high resolution ($\sim 100 \text{ pc}$) ALMA observations of the 350 GHz band including HCN ($J=4-3$) and HCO^+ ($J=4-3$) emissions from the type-1 Seyfert nucleus of NGC 1097. The conclusions are summarized as follows:

- The HCN ($J=4-3$) to CS ($J=7-6$) and HCN ($J=4-3$) to HCO^+ ($J=4-3$) integrated intensity ratios are higher in AGNs than in SB environments. Although the sample is small, we consider these line ratios are effective discriminator between AGN and SB activities, and thus constructed a tentative diagnostic diagram.
- We ran non-LTE simulations by RADEX to constrain the excitation parameters of the HCN and HCO^+ lines. The χ^2 tests using the $J=4-3$ and $3-2$ lines show that these emissions come from dense ($10^{4.5} \leq n_{\text{H}_2} [\text{cm}^{-3}] \leq 10^6$), and hot ($70 \leq T_{\text{kin}} [\text{K}] \leq 550$) environments, and $[\text{HCN}]/[\text{HCO}^+]$ is estimated to be 4–20.
- We introduce a chemical layouts based on a high temperature chemistry to explain the observed HCN -enhancement, although the heating source is still not clear. Another heating source separate from the radiative heating, such as shocks associated with the AGN, is suggested to exist.

We confirmed that multi- J modeling including HCN and HCO^+ by using ALMA is a powerful tool to investigate the physical/chemical properties of dense molecular medium around an AGN. We will apply this method to other key

IZUMI ET AL.

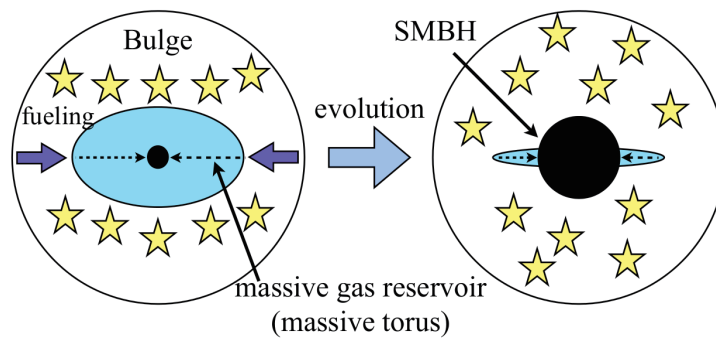


Figure 3. Schematic picture of the coevolution of the supermassive black hole and the surrounding massive gas reservoir (massive torus). The gas mass to black hole mass ratio, $M_{\text{gas}}/M_{\text{BH}}$, is expected to decrease as the black hole evolves.

molecules and other galaxies in future ALMA observations, which can be combined with *SPICA* to produce synergistic effects. For example, Kawakatu et al. (2007) predicted the existence of massive gas reservoir (massive gas torus) with a mass of $\sim 10^8\text{--}10^9 M_{\odot}$ extending over a ~ 100 pc scale around the central supermassive black hole (SMBH) in galaxies. They concluded that the gas mass to black hole mass ratio, and the geometry of the massive torus reflect the growth history of SMBH (Figure 3). To test this scheme, the fast survey speed of *SPICA* will play an important role in finding AGNs with various activities at various eras by using optical/IR diagnostic method. On the other hand, ALMA can follow up those galaxies in detail thanks to its extremely high angular resolution and sensitivity, and can measure the mass and the geometry of the expected massive gas tori. Clearly, the synergy of these two telescopes is the key to revealing the evolutionary history of SMBHs, and then to shedding a light on the dark side of the universe.

This paper makes use of the following ALMA data: ADS/JAO. ALMA#2011.0.00108.S. ALMA is a partnership of ESO (representing its member states), NSF (USA) and NINS (Japan), together with NRC (Canada) and NSC and ASIAA (Taiwan), in co-operation with the Republic of Chile. The Joint ALMA Observatory is operated by ESO, AUI/NRAO and NAOJ.

REFERENCES

- Bayet, E., Aladro, R., Martín, S., et al. 2009, *ApJ*, 707, 126
 Bayet, E., Lintott, C., Viti, S., et al. 2008, *ApJL*, 685, L35
 Harada, N., Herbst, E., & Wakelam, V. 2010, *ApJ*, 721, 1570
 Hsieh, P.-Y., Ho, P. T. P., Kohno, K., et al. 2012, *ApJ*, 747, 90
 Imanishi, M., & Nakanishi, K. 2013, *AJ*, 146, 47
 Imanishi, M., Nakanishi, K., Kuno, N., & Kohno, K. 2004, *AJ*, 128, 2037
 Iono, D., Saito, T., Yun, M. S., et al. 2013, *PASJ*, 65, L7
 Izumi, T., Kohno, K., Martín, S., et al. 2013, *PASJ*, 65, 100
 Kawakatu, N., Andreani, P., Granato, G. L., & Danese, L. 2007, *ApJ*, 663, 924
 Knudsen, K. K., Walter, F., Weiss, A., et al. 2007, *ApJ*, 666, 156
 Kohno, K. 2005, in *The Evolution of Starbursts*, edited by S. Hüttmeister, E. Manthey, D. Bomans, & K. Weis, vol. 783 of *American Institute of Physics Conference Series*, 203
 Kohno, K., Ishizuki, S., Matsushita, S., et al. 2003, *PASJ*, 55, L1
 Kormendy, J., & Ho, L. C. 2013, *ARA&A*, 51, 511
 Lahuis, F., Spoon, H. W. W., Tielens, A. G. G. M., et al. 2007, *ApJ*, 659, 296
 Nemmen, R. S., Storchi-Bergmann, T., Yuan, F., et al. 2006, *ApJ*, 643, 652
 Pérez-Beaupuits, J. P., Spaans, M., van der Tak, F. F. S., et al. 2009, *A&A*, 503, 459
 Sakamoto, K., Aalto, S., Evans, A. S., et al. 2010, *ApJL*, 725, L228
 Schilke, P., Groesbeck, T. D., Blake, G. A., & Phillips, T. G. 1997, *ApJS*, 108, 301
 Seaquist, E. R., & Frayer, D. T. 2000, *ApJ*, 540, 765
 Spoon, H. W. W., Keane, J. V., Tielens, A. G. G. M., et al. 2001, *A&A*, 365, L353
 van der Tak, F. F. S., Black, J. H., Schöier, F. L., et al. 2007, *A&A*, 468, 627